IEEE Access
Multidisciplinary : Rapid Review : Open Access Journal

Received March 30, 2020, accepted April 11, 2020, date of publication April 14, 2020, date of current version April 29, 2020.

*Digital Object Identifier 10.1109/ACCESS.2020.2987976*

# Neural Network-Based Error-Tracking Iterative Learning Control for Tank Gun Control Systems With Arbitrary Initial States

**QIYAO YANG[1], QIUZHEN YAN[2], JIANPING CAI[1], JINGHUA TIAN[2], AND XIAOHUI GUAN[2]**

[1]School of Electrical Engineering, Zhejiang University of Water Resources and Electric Power, Hangzhou 310018, China
[2]College of Information Engineering, Zhejiang University of Water Resources and Electric Power, Hangzhou 310018, China

Corresponding author: Qiuzhen Yan (zjhzyqz@gmail.com)

This work was supported in part by the National Natural Science Foundation of China under Grant 61573322, in part by the Scientific Research Project of the Water Conservancy Department of Zhejiang Province under Grant RC1858, and in part by the Zhejiang Province Welfare Technology Applied Research Project under Grant LGF20F020007.

**ABSTRACT** In this paper, a novel neural network-based error-track iterative learning control scheme is proposed to tackle trajectory tracking problem for tank gun control systems. Firstly, the system modeling for tank gun control systems is introduced as a preparation of controller design. Then, the reference error trajectory is constructed to deal with the nonzero initial error of iterative learning control. The adaptive iterative learning controller for tank gun control systems is designed by using Lyapunov approach. Adaptive learning neural network is adopted to approximate nonlinear uncertainties, with robust control technique being used compensate the approximation error and external disturbances. As the iteration number increases, the system error can follow the desired error trajectory over the whole time interval, which makes the system state accurately track the reference error trajectory during the predetermined part time interval. Numerical simulations demonstrate the effectiveness of the proposed iterative learning control scheme.

**INDEX TERMS** Tank gun control systems, iterative learning control, neural network, Lyapunov approach.

## I. INTRODUCTION

Iterative learning control (ILC) is a proper control technique for those uncertain systems which repetitively operating over finite time intervals [1]. Due to its high-precision tracking performance despite the lack of prior knowledge on system model, ILC has earned a great deal of interest.

In the past two decades, adaptive ILC has been a hot issue in ILC field for at least two reasons. Firstly, comparing with contraction-mapping ILC, adaptive ILC is capable of handling non-global Lipschitz continuous uncertainties.

Secondly, adaptive ILC may be used in controller design for parametric uncertain systems, conveniently. Early results on adaptive ILC focus on estimating and attenuating time-invariant uncertainties over a finite time interval, by using differential learning approaches [2]. Later on, difference learning approaches are explored to deal with time-varying but iteration-invariant uncertainties [3]. Along with the deep development of study, more complicated parametric uncertainties has been investigated in the field of adaptive ILC. Yin *et al.* investigated the high-order internal model strategy to estimate a class of iteration-varying parametric uncertainties [4]. Ye xudong developed an adaptive ILC law for a class of nonlinear systems, in which, the period length of disturbance is unknown [5]. In addtition, the adaptive ILC developments for nonparametric systems have been carried out in recent years [6], [7]. For more detail about the recent development in the related fields, see [8]–[12].

On the other hand, tank is a kind of offensive and defensive weapon in modern battlefields for enhancing soldiers' surviving ability and the efficiency of artillery firepower.

While in fighting, tank gun control systems (TGCSs) need accomplish a launch mission under the circumstance with friction, uncertainties and external disturbances. The researches on trajectory-tracking control for TGCSs have been carried out for ages, and the main related schemes have been proposed by using variable structure control [13], optimal control [14], [15], PID control control [16], adaptive

The associate editor coordinating the review of this manuscript and approving it for publication was Haibin Sun.

control [17], [18] and adaptive robust control [19]. The above researches have promoted the development of control technique for TGCSs, but the high-precision control for TGCSs is still an issue to be solved. In order to obtain better control performance, in recent years, researchers have explored the ILC control development for TGCSs [20], [21]. As mentioned above, since the complicated application scenarios and the difficulties in system modeling, there exists complicated uncertainties in TGCSs, such as parametric uncertainties, nonparametric uncertainties and random perturbations. In [22] and [23], disturbance observer were designed to approximate uncertainties. In [24] and [25], an adaptive fuzzy system and an adaptive neural network were adopted to approximate the uncertainties and disturbances in TGCSs, respectively.

The zero-initial error condition is an obstacle in the ILC design for TGCSs. In traditional ILC algorithms, there usually assume that the initial system error must be zero at each iteration, which is called the initial problem of ILC [26]–[28]. Otherwise, a slight initial error may lead to the divergence of tracking error. In industrial applications, achieving such a zero-error initial resetting at each iteration is actually an impossible task. Therefore, relaxing the zero-error resetting condition is very significant to broaden the application fields of ILC. In recent years, through continuous explorations, a few solutions have been proposed, such as time-varying boundary layer [29], [30], error-tracking strategy [31]- [33], initial rectifying action [34]- [36]. In [21], alignment condition is used as a solution to remove the zero initial error condition for the ILC design in TGCSs, and the algorithm can work well in the TGCSs whose reference trajectories are smoothly closed. In [20], an error-tracking ILC algorithm was proposed for TGCSs whose initial velocity is allowed to be any bounded value, but whose initial acceleration error is assumed to be zero. Therefore, it is necessary to carry out further research in adaptive iterative learning controller design for TGCSs with both nonzero initial velocity error and nonzero initial acceleration error.

Motivated by the above discussions, this work focuses on trajectory-tracking problem for TGCSs with arbitrary initial states. The adaptive iterative learning controller is designed by using Lyapunov approach, with adaptive learning neural network being constructed to approximate uncertainties in TGCSs. Compared to the existing results, the main contributions of this work mainly lie in the several fields as follows:

(1) With reference error trajectory is constructed for dealing with nonzero initial errors, the error-tracking strategy is adopted to solve the initial problem of ILC for TGCSs.

(2) An adaptive learning radial basis function (RBF) neural network is used to approximate uncertainties in tank gun servo systems. The optimal weight of neural network is estimated by using difference learning method.

(3) A Lyapunov functional is constructed for the controller design, and the corresponding convergence analysis of closed loop system is given.

The rest of this paper is organized as follows. The system model of TGCSs, the control objective and the detailed construction process of reference error trajectory are addressed in Section 2. The adaptive iterative learning controller design is presented in Section 3, with the corresponding convergence analysis given in Section 4. In Section 5, an illustrative example is provided to demonstrate the effectiveness of the proposed ILC scheme. Section 6 concludes this paper.

## II. PROBLEM FORMULATION

Nowadays, all-electric TGCSs have become the mainstream of development of TGCSs. Comparing to traditional electro-hydraulic/all-hydraulic TGCSs, all-electric TGCSs have simpler structure and higher efficiency. In all-electric TGCS, the direction adjustments of turret and gun, including horizontal-direction adjustments and vertical-direction adjustments, can be fulfilled by using by motor drives. Fig. 1 shows the structure of vertical servo system of all-electrical tank gun. The main parts of controlled device are AC motor, speed reducer and barrel.

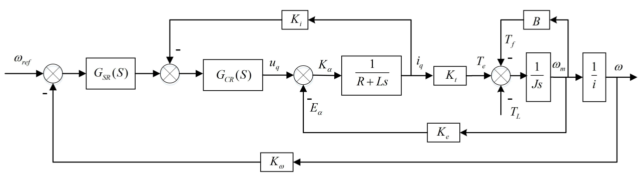


**FIGURE 1. Structure diagram of all-electrical tank gun vertical servo system.**

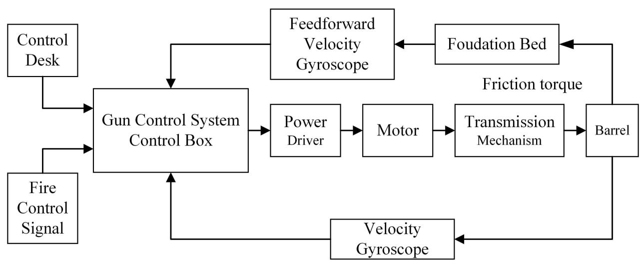


**FIGURE 2. Transfer function block diagram of tank gun AC servo system.**

The block diagram of tank gun AC servo system is presented in Fig. 2, where $\omega_{ref}$ and $\omega$ represent the desired angular velocity and the real angular velocity of the cannon, repectively. $G_{SR}(s)$ and $G_{CR}(s)$ are the velocity regulator and the current regulator, respectively. $u_q$ is the output voltage of the current loop. $R$ and $L$ represent the resistance and the inductance of motor armature circuit, respectively. $K_a$ is the amplifier gain. $E_a$ is the armature back electromotive force of motor. $K_i$ is the current feedback coefficient of $q$ axis. $K_t$ is the motor torque factor. $K_e$ denotes the electric torque coefficient. $T_e$, $T_L$ and $T_f$ are the motor torque, load torque disturbance and friction torque disturbance, respectively. $K_\omega$ is the angular velocity feedback coefficient of cannon. $J$ is the total moment of inertia to the rotor. $B$ is the viscous friction coefficient. $i$ is the moderating ratio. $s$ denotes the Laplace operator.

From Fig. 2, we can obtain

$$\begin{cases} \dot{i}_q = -\frac{R}{L}i_q - \frac{K_e i}{L}\omega + \frac{K_a}{L}u_q, \\ \dot{\omega} = \frac{K_t}{Ji}i_q - \frac{1}{Ji}T_{Ls} \end{cases} \tag{1}$$

where $T_{Ls} = T_L + T_f$.

Define $x_1 = \omega, x_2 = \dot{\omega}$. Then, from (1), the dynamics of TGCSs at the $k$th iteration can be described as

$$\begin{cases} \dot{x}_{1,k} = x_{2,k}, \\ \dot{x}_{2,k} = -\frac{R}{L}x_{2,k} - \frac{K_t K_e}{LJ}x_{1,k} + \frac{K_a K_t}{LJi}u_{q,k} \\ +\Delta f(\boldsymbol{x}_k, t), \end{cases} \tag{2}$$

where, $k(= 0, 1, 2, 3, \cdots)$ is the iteration number, $\boldsymbol{x}_k = [x_{1,k}, x_{2,k}]^T$, $\Delta f(\boldsymbol{x}_k, t) = -\frac{R}{LJi}T_{Ls,k} - \frac{1}{Ji}\dot{T}_{Ls,k}$. Without loss of generality, we assume $\Delta f(\boldsymbol{x}_k, t) = f_1(\boldsymbol{x}_k) + f_2(\boldsymbol{x}_k, t)$, where $f_1(\boldsymbol{x}_k)$ is the continuous part with respect to $\boldsymbol{x}_k$, and $f_2(\boldsymbol{x}_k, t)$ represents the sum of discontinuous but bounded perturbations. In addition, the parameters in (2), including $R, L, K_t, K_e, K_a, K_t, J$ and $i$, are all assumed to be unknown constants.

Letting $\boldsymbol{e}_k(t) = [e_{1,k}(t), e_{2,k}(t)]^T = \boldsymbol{x}_k(t) - \boldsymbol{x}_d(t)$, from (2), we can obtain

$$\begin{cases} \dot{e}_{1,k} = e_{2,k}, \\ \dot{e}_{2,k} = -\frac{R}{L}x_{2,k} - \frac{K_t K_p}{LJ}x_{1,k} + \frac{K_a K_t}{LJi}u_{q,k} \\ \quad + \Delta f(\boldsymbol{x}_k, t) - \ddot{x}_d. \end{cases} \tag{3}$$

In this work, we want to drive $\boldsymbol{e}_k(t)$ to follow $\boldsymbol{e}^r_k(t) = [e^r_{1,k}(t), e^r_{2,k}(t)]^T$ over $[0, T]$, which actually is a bridge to make $\boldsymbol{x}_k(t)$ track $\boldsymbol{x}_d(t)]^T$ over $[T_1, T]$. Here, $T_1$ is a time point between 0 and $T$, whose value is predetermined according to the need of practical application.

The reference error trajectory $\boldsymbol{e}^r_k(t)$ is constructed as follows. For $0 \le t < T_1$,

let $e^r_{1,k}(t) = 0, e^r_{2,k}(t) = 0$. For $T_1 \le t \le T$, let

$$\begin{aligned} e^r_{1,k}(t) =& \ a_{0,k} + a_{1,k}t + a_{2,k}t^2 + a_{3,k}t^3 + a_{4,k}t^4 \\ & + a_{5,k}t^5, \\ e^r_{2,k}(t) =& \ a_{1,k} + 2a_{2,k}t + 3a_{3,k}t^2 + 4a_{4,k}t^3 \\ & + 5a_{5,k}t^4, \end{aligned}$$

where, $a_{0,k} = e_{1,k}(0)$, $a_{1,k} = e_{2,k}(0)$, $a_{2,k} = 0$,

$$\begin{pmatrix} a_{3,k} \\ a_{4,k} \\ a_{5,k} \end{pmatrix} = \begin{pmatrix} T_1^3 & T_1^4 & T_1^5 \\ 3T_1^2 & 4T_1^3 & 5T_1^4 \\ 6T_1 & 12T_1^2 & 20T_1^3 \end{pmatrix}^{-1} \times \begin{pmatrix} -a_{0,k} - a_{1,k}T_1 - a_{2,k}T_1^2 \\ -a_{1,k} - 2a_{2,k}T_1 \\ -2a_{2,k} \end{pmatrix}.$$

From the above constructions, we can see that if $\boldsymbol{e}_k(t)$ can follow $\boldsymbol{e}^r_k(t)$ over $[0, T]$, then the precise tracking from $\boldsymbol{x}_k(t)$ to $\boldsymbol{x}_d(t)$ may be achieved during $[T_1, T]$.

Let $z_{1,k} = e_{1,k} - e^r_{1,k}, z_{2,k} = e_{2,k} - e^r_{2,k}$ and $s_{z,k} = \alpha z_{1,k} + z_{2,k}$, with $\alpha > 0$. According to the above-mentioned construction method, $z_{1,j}(0) = e_{1,j}(0) - e^r_{1,j}(0) = 0$ and $z_{2,j}(0) = e_{2,j}(0) - e^r_{2,j}(0) = 0$ hold for $j = 0, 1, 2, \cdots, k$, which leads to

$$s_{z,j}(0) = \alpha z_{1,j}(0) + z_{2,j}(0) = 0, \quad j = 0, 1, 2, \cdots, k. \tag{4}$$

From (4), we can deduce eqtuation (25), which plays an important role in the convergence analysis of adaptive ILC design.

## III. CONTROL SYSTEM DESIGN

It follows from (3) that

$$\begin{cases} \dot{z}_{1,k} = z_{2,k}, \\ \dot{z}_{2,k} = -\frac{R}{L}x_{2,k} - \frac{K_t K_p}{LJ}x_{1,k} + \frac{K_a K_t}{LJi}u_{q,k} + f_1(\boldsymbol{x}_k) \\ \quad + f_2(\boldsymbol{x}_k, t) - \ddot{x}_d - \dot{e}^r_{2,k} \end{cases}$$

and

$$\begin{aligned} \dot{s}_{z,k} = \alpha z_{2,k} - \frac{R}{L}x_{2,k} - \frac{K_t K_p}{LJ}x_{1,k} + \frac{K_a K_t}{LJi}u_{q,k} \\ + f_1(\boldsymbol{x}_k) + f_2(\boldsymbol{x}_k, t) - \ddot{x}_d - \dot{e}^r_{2,k}. \end{aligned} \tag{5}$$

Let $h \triangleq \frac{K_a K_t}{LJi}$. Taking the derivative of $V_k = \frac{1}{2h}s^2_{z,k}$ with respect to time yields

$$\begin{aligned} \dot{V}_k = s_{z,k}[\frac{1}{h}(\alpha z_{2,k} - \ddot{x}_d - \dot{e}^r_{2,k}) - \frac{R}{hL}x_{2,k} - \frac{K_t K_p}{hLJ}x_{1,k} \\ + u_{q,k} + \frac{1}{h}f_1(\boldsymbol{x}_k) + \frac{1}{h}f_2(\boldsymbol{x}_k, t)]. \end{aligned} \tag{6}$$

Then, by adopting radial basis function (RBF) neural network to approximate

$$\frac{1}{h}(\alpha z_{2,k} - \ddot{x}_d - \dot{e}^r_{2,k}) - \frac{R}{hL}x_{2,k} - \frac{K_t K_p}{hLJ}x_{1,k} + \frac{1}{h}f_1(\boldsymbol{x}_k),$$

we design the ILC law as

$$u_{q,k} = -\gamma_1 s_{z,k} - \boldsymbol{\theta}^T_k(t)\boldsymbol{\phi}(X_k) - \frac{2\eta_k s_{z,k}}{|s_{z,k}| + \varepsilon} \tag{7}$$

and adaptive learning laws as

$$\boldsymbol{\theta}_k = \mathrm{sat}_{\underline{\theta},\bar{\theta}}(\boldsymbol{\theta}_{k-1}) + \gamma_2 s_{z,k}\boldsymbol{\phi}(\boldsymbol{X}_k), \quad \boldsymbol{\theta}_{-1} = 0, \tag{8}$$

$$\eta_k = \mathrm{sat}_{0,\bar{\eta}}(\eta_{k-1}) + \gamma_3|s_{z,k}|, \quad \eta_{-1} = 0. \tag{9}$$

where, $\gamma_1 > 0, \gamma_2 > 0, \gamma_3 > 0, \varepsilon > 0, \boldsymbol{\theta}^T_k(t)\boldsymbol{\phi}(X_k)$ and $\eta_k$ are used to approximate

$$\begin{aligned} \boldsymbol{\theta}^{*T}(t)\boldsymbol{\phi}(X_k) = \frac{1}{h}(\alpha z_{2,k} - \ddot{x}_d - \dot{e}^r_{2,k}) - \frac{R}{hL}x_{2,k} \\ - \frac{K_t K_p}{hLJ}x_{1,k} + \frac{1}{h}f_1(\boldsymbol{x}_k) - \epsilon(X_k) \end{aligned} \tag{10}$$

and

$$\eta(t) = \sup\left(|\frac{1}{h}f_2(\boldsymbol{x}_k, t) + \epsilon(X_k)|\right), \tag{11}$$

respectively. In (10) and (11), $\boldsymbol{\theta}^*(t)$ is the optimal weight of neural network, $\epsilon(\boldsymbol{X}_k)$ is the approximation error,

$\boldsymbol{X}_k = [e_{1,k}^*, e_{2,k}^*, e_{1,k}, e_{2,k}, x_d, \dot{x}_d, \ddot{x}_d]^T$ and $\boldsymbol{\phi}(X_k) = [\phi_{1,k}, \phi_{2,k}, \cdots, \phi_{m,k}]^T$ with

$$\phi_{j,k} = \mathrm{e}^{-\frac{\|\boldsymbol{X}_k - \boldsymbol{c}_j\|^2}{2b_j^2}}, \quad j = 1, 2, \cdots, m. \tag{12}$$

In (12), $\boldsymbol{c}_j$ and $b_j$ are the center and the width of the receptive field, respectively. In learning laws (8) and (9), the definition of saturation functions is given as follows. For scalar $\hat{a}$,

$$\mathrm{sat}_{\underline{a},\bar{a}}(\hat{a}) \triangleq \begin{cases} \bar{a} \hat{a} > \bar{a} \\ a \ \underline{a} \le \hat{a} \le \bar{a} \\ \underline{a} \ \hat{a} < \underline{a}. \end{cases}$$

For a vector $\hat{\boldsymbol{a}} = [\hat{a}_1, \hat{a}_2, \cdots, \hat{a}_m] \in \boldsymbol{R}^p$, $\mathrm{sat}_{\underline{a},\bar{a}}(\hat{\boldsymbol{a}}) \triangleq \left[\mathrm{sat}_{\underline{a},\bar{a}}(\hat{a}_1), \mathrm{sat}_{\underline{a},\bar{a}}(\hat{a}_2), \cdots, \mathrm{sat}_{\underline{a},\bar{a}}(\hat{a}_p)\right]^T$.

For brevity, in the rest of this paper, $\boldsymbol{\phi}(X_k)$ is abbreviated as $\boldsymbol{\phi}_k$, and arguments are sometimes omitted while no confusion occurs.

## IV. CONVERGENCE ANALYSIS

*Theorem 1:* For the tank servo dynamic system (2), the adaptive learning controller specified by equations (7)-(9) ensures that all signals in the closed loop system are bounded and $|s_{z,k}(t)| \le \varepsilon$ holds $\forall t \in [0, T]$ as the iteration number increases, which means

$$|e_{1,k}(t)| < \frac{\varepsilon}{\alpha}, \quad t \in [T_1, T] \tag{13}$$

and

$$|e_{2,k}(t)| < 2\varepsilon, \quad t \in [T_1, T]. \tag{14}$$

*Proof:* The proof consists of three parts. Part 1 derives the difference of the Lyapunov functional $L_k$. Part 2 proves the Lyapunov functional $L_k$ is bounded for $k = 0$. The perfect tracking performance and the boundedness of all signals in the closed loop system are shown in Part 3.

Part 1. Difference of $L_k$

Substituting (7) into (6), we obtain

$$\dot{V}_k \le -\gamma_1 s_{z,k}^2 + s_{z,k}[\boldsymbol{\theta}^{*T}(t)\boldsymbol{\phi}(X_k) - \boldsymbol{\theta}_k^T(t)\boldsymbol{\phi}(X_k)] + |s_{z,k}|\eta(t) - \frac{2\eta_k s_{z,k}^2}{|s_{z,k}| + \varepsilon} \tag{15}$$

Define $\tilde{\eta}_k = \eta - \eta_k$. While $|s_{z,k}| \ge \varepsilon$,

$$\begin{aligned} |s_{z,k}|\eta - \frac{2\eta_k s_{z,k}^2}{|s_{z,k}| + \varepsilon} &\le |s_{z,k}|\eta(t) - \eta_k|s_{z,k}| \\ &= \tilde{\eta}_k|s_{z,k}|. \end{aligned} \tag{16}$$

Combining (15) with (16), we get

$$\dot{V}_k \le -\gamma_1 s_{z,k}^2 + s_{z,k}\tilde{\boldsymbol{\theta}}_k^T\boldsymbol{\phi}_k + |s_{z,k}|\tilde{\eta}_k, \tag{17}$$

where $\tilde{\boldsymbol{\theta}}_k = \boldsymbol{\theta} - \boldsymbol{\theta}_k$. From (17), we have

$$V_k(t) \le V_k(0) - \gamma_1 \int_0^t s_{z,k}^2 d\tau + \int_0^t s_{z,k}\tilde{\boldsymbol{\theta}}_k^T\boldsymbol{\phi}_k d\tau + \int_0^t |s_{z,k}|\tilde{\eta}_k d\tau. \tag{18}$$

Define a candidate Lyapunov functional at the $k$th iteration as

$$L_k = V_k + \frac{1}{2\gamma_2}\int_0^t \tilde{\boldsymbol{\theta}}_k^T\tilde{\boldsymbol{\theta}}_k d\tau + \frac{1}{2\gamma_3}\int_0^t \tilde{\eta}_k^2 d\tau, \tag{19}$$

where, $k = 0, 1, 2, 3, \cdots$. While $k > 0$ and $|s_{z,k}| \ge \varepsilon$, from (18) and (19), we have

$$\begin{aligned} &L_k - L_{k-1} \\ &\le V_k(0) - \gamma_1 \int_0^t s_{z,k}^2 d\tau + \int_0^t s_{z,k}\tilde{\boldsymbol{\theta}}_k^T\boldsymbol{\phi}_k d\tau + \int_0^t |s_{z,k}|\tilde{\eta}_k d\tau \\ &\quad -V_{k-1} + \frac{1}{2\gamma_2}\int_0^t (\tilde{\boldsymbol{\theta}}_k^T\tilde{\boldsymbol{\theta}}_k - \tilde{\boldsymbol{\theta}}_{k-1}^T\tilde{\boldsymbol{\theta}}_{k-1}) d\tau \\ &\quad + \frac{1}{2\gamma_3}\int_0^t (\tilde{\eta}_k^2 - \tilde{\eta}_{k-1}^2) d\tau \end{aligned} \tag{20}$$

As the appendix $I$ of Reference [37] addressed, $(a - \hat{a})^2 \ge (a - \mathrm{sat}_{\underline{a},\bar{a}}(\hat{a}))^2$ holds. By this property, from (8) and (9), we obtain

$$\begin{aligned} &\frac{1}{2\gamma_2}(\tilde{\boldsymbol{\theta}}_k^T\tilde{\boldsymbol{\theta}}_k - \tilde{\boldsymbol{\theta}}_{k-1}^T\tilde{\boldsymbol{\theta}}_{k-1}) + s_{z,k}\tilde{\boldsymbol{\theta}}_k^T\boldsymbol{\phi}_k \\ &\quad \le \frac{1}{2\gamma_2}[(\boldsymbol{\theta} - \boldsymbol{\theta}_k)^T(\boldsymbol{\theta} - \boldsymbol{\theta}_k) - (\boldsymbol{\theta} - \mathrm{sat}_{\underline{\theta},\bar{\theta}}(\boldsymbol{\theta}_{k-1}))^T(\boldsymbol{\theta} \\ &\quad\quad -\mathrm{sat}_{\underline{\theta},\bar{\theta}}(\boldsymbol{\theta}_{k-1}))] + s_{z,k}\tilde{\boldsymbol{\theta}}_k^T\boldsymbol{\phi}_k \\ &\quad \le \frac{1}{2\gamma_2}(2\boldsymbol{\theta} - \boldsymbol{\theta}_k - \mathrm{sat}_{\underline{\theta},\bar{\theta}}(\boldsymbol{\theta}_{k-1}))^T(\mathrm{sat}_{\underline{\theta},\bar{\theta}}(\boldsymbol{\theta}_{k-1}) - \boldsymbol{\theta}_k) \\ &\quad\quad + s_{z,k}\tilde{\boldsymbol{\theta}}_k^T\boldsymbol{\phi}_k \\ &\quad \le \frac{1}{\gamma_2}(\boldsymbol{\theta} - \boldsymbol{\theta}_k)^T(\mathrm{sat}_{\underline{\theta},\bar{\theta}}(\boldsymbol{\theta}_{k-1}) - \boldsymbol{\theta}_k) + s_{z,k}\tilde{\boldsymbol{\theta}}_k^T\boldsymbol{\phi}_k \\ &\quad = 0 \end{aligned} \tag{21}$$

and

$$\begin{aligned} &\frac{1}{2\gamma_3}(\tilde{\eta}_k^2 - \tilde{\eta}_{k-1}^2) + |s_{z,k}|\tilde{\eta}_k \\ &\quad \le \frac{1}{2\gamma_3}(2\eta - \eta_k - \mathrm{sat}_{0,\bar{\eta}}(\eta_{k-1}))(\mathrm{sat}_{0,\bar{\eta}}(\eta_{k-1}) - \eta_k) \\ &\quad\quad + |s_{z,k}|\tilde{\eta}_k \\ &\quad \le \frac{1}{\gamma_3}(\eta - \eta_k)(\mathrm{sat}_{0,\bar{\eta}}(\eta_{k-1}) - \eta_k) + |s_{z,k}|\tilde{\eta}_k \\ &\quad = 0, \end{aligned} \tag{22}$$

respectively. Substituting (21) and (22) into (20) leads to

$$\begin{aligned} L_k - L_{k-1} &\le V_k(0) - \gamma_1 \int_0^t s_{z,k}^2 d\tau - V_{k-1} \\ &\le V_k(0) - V_{k-1}, \end{aligned} \tag{23}$$

which further implies

$$L_k(t) \le \sum_{j=1}^k V_j(0) + L_0(t) - \frac{1}{2h}\sum_{j=0}^{k-1} s_{z,j}^2(t). \tag{24}$$

As addressed in (4), $s_{z,j}(0) = 0$ holds for $j = 0, 1, 2, \cdots, k$. Hence, we can easily draw a conclusion that

$$V_k(0) = 0 \tag{25}$$

and

$$\sum_{j=1}^{k} V_j(0) = 0 \tag{26}$$

hold for $j = 0, 1, 2, \cdots, k$. Then, from (24) and (26), we have

$$L_k(t) \le L_0(t) - \frac{1}{2h}\sum_{j=0}^{k-1} s_{z,j}^2(t) \tag{27}$$

*Remark 1:* According to the construction strategy given in Section 2, we can see that (25) holds, which is a sufficient condition for deducing (26). Further, (26) helps to deduce (27). In traditional adaptive ILC design, usually, the candidate Lyapunov function is chosen as

$$V_{e,k} = \frac{1}{2}s_k^2, \tag{28}$$

where $s_k = \alpha e_{1,k} + e_{2,k}$. Since $s_k(0) \neq 0$ and $V_{e,k}(0) \neq 0$, we can not draw a conclusion similar to (27). Hence, $V_{e,k}$ is not a suitable candidate Lyapunov function for ILC design.

Part 2. Finiteness of $L_0(t)$

Taking the time derivative of $L_0 = V_0 + \frac{1}{2\gamma_2}\int_0^t \tilde{\boldsymbol{\theta}}_0^T\tilde{\boldsymbol{\theta}}_0 d\tau + \frac{1}{2\gamma_3}\int_0^t \tilde{\eta}_{\epsilon,0}^2 d\tau$, we have

$$\begin{aligned}
\dot{L}_0 &= -\gamma_1 s_{z,0}^2 + s_{z,0}\tilde{\boldsymbol{\theta}}_0^T\boldsymbol{\phi}_0 + |s_{z,0}|\tilde{\eta}_0 + \frac{1}{2\gamma_2}\tilde{\boldsymbol{\theta}}_0^T\tilde{\boldsymbol{\theta}}_0 \\
&\quad + \frac{1}{2\gamma_3}\tilde{\eta}_0^2 \\
&= -\gamma_1 s_{z,0}^2 + \frac{\boldsymbol{\theta}_0^T}{\gamma_2}(\boldsymbol{\theta}^* - \boldsymbol{\theta}_0) + \frac{1}{\gamma_3}\eta_0(\eta - \eta_0) \\
&\quad + \frac{1}{2\gamma_2}(\boldsymbol{\theta}^* - \boldsymbol{\theta}_0)^T(\boldsymbol{\theta}^* - \boldsymbol{\theta}_0) + \frac{1}{2\gamma_3}(\eta - \eta_0)^2 \\
&= -\gamma_1 s_{z,0}^2 + \frac{1}{2\gamma_2}(\boldsymbol{\theta}^* - \boldsymbol{\theta}_0)^T(\boldsymbol{\theta}^* + \boldsymbol{\theta}_0) \\
&\quad + \frac{1}{2\gamma_3}(\eta + \eta_0)(\eta - \eta_0) \\
&= -\gamma_1 s_{z,0}^2 + \frac{1}{2\gamma_2}(\boldsymbol{\theta}^{*T}\boldsymbol{\theta}^* - \boldsymbol{\theta}_0^T\boldsymbol{\theta}_0) + \frac{1}{2\gamma_3}(\eta^2 - \eta_0^2) \\
&\le -\gamma_1 s_{z,0}^2 + \frac{1}{2\gamma_2}\boldsymbol{\theta}^{*T}\boldsymbol{\theta}^* + \frac{1}{2\gamma_3}\eta^2.
\end{aligned} \tag{29}$$

Obviously, there exists a large enough positive constant $\varrho$, which satisfies $\varrho \ge \sup(\frac{1}{2\gamma_2}\boldsymbol{\theta}^{*T}\boldsymbol{\theta}^* + \frac{1}{2\gamma_3}\eta^2)$ and $\dot{L}_0 \le -\gamma_1 s_{z,0}^2 + \varrho \le \varrho$. Therefore, from (29), we can conclude

$$L_0(t) \le L_0(0) + \varrho t = \varrho T, \quad \forall t \in [0, T]. \tag{30}$$

Part 3. Convergence of tracking error

By the definition of Lyapunov functional, we know $L_0(t) \ge 0$ and $L_k(t) \ge 0$. Note that $|s_{z,k}| \ge \varepsilon$ is a precondition of (27). If $|s_{z,k}| \ge \varepsilon$ holds as the iteration number increases, then combining (27) with (30) may lead to $L_k(t) < 0$, which is in contradiction with the nonnegativity of $L_k(t)$. Hence, we conclude that $|s_{z,k}(t)| < \varepsilon$, $t \in [0, T]$ as the iteration number increases.

On the basis of $\dot{z}_{1,k} + \alpha z_{1,k} = s_{z,k}$, we have,

$$\frac{d}{dt}(\mathrm{e}^{\alpha t}z_{1,k}) = \mathrm{e}^{\alpha t}s_{z,k}, \tag{31}$$

Calculating the definite integrals on both sides of (31) from 0 to $t$ yields

$$\mathrm{e}^{\alpha t}z_{1,k}(t) - \mathrm{e}^{0}z_{1,k}(0) = \int_0^t \mathrm{e}^{\alpha\tau}s_{z,k}(\tau)d\tau. \tag{32}$$

Note that $z_{j,k}(0) = 0$ holds. From (32), we get

$$|z_{1,k}(t)| \le \frac{\mathrm{e}^{-\alpha t}}{\alpha}(\mathrm{e}^{\alpha t} - 1)\varepsilon < \frac{\varepsilon}{\alpha}, \quad t \in [0, T] \tag{33}$$

which implies that

$$|e_{1,k}(t)| < \frac{\varepsilon}{\alpha}, \quad t \in [T_1, T]. \tag{34}$$

In addition, from (33) and by the definition of $s_{z,k}$, we have

$$|z_{2,k}(t)| \le |s_{z,k}(t)| + \alpha|z_{1,k}(t)| < 2\varepsilon, \quad t \in [0, T], \tag{35}$$

which gives that

$$|e_{2,k}(t)| < 2\varepsilon, \quad t \in [T_1, T]. \tag{36}$$

Therefore, by choosing proper $\varepsilon$, we can get the desired control precision for closed loop TGCSs. Usually, $\varepsilon$ may be set between 0.001 and 0.1, and $\alpha$ may be set between 1 and 5. ■

In the learning law design of this work, we adopt the partial saturation strategy to guarantee the boundedness of the parameters estimation. Comparing to the unsaturation learning law design, the proposed saturation learning scheme own higher security and reliability.

*Remark 2:* If the control law (7) is substituted by

$$u_{q,k} = -\gamma_1 s_{z,k} - \boldsymbol{\theta}_k^T(t)\boldsymbol{\phi}(X_k) - \eta_k \operatorname{sgn}(s_{z,k}), \tag{37}$$

then $|s_{z,k}| \to 0$ can hold as $k \to +\infty$. However, chattering phenomenon will happen due to using sign function.

## V. NUMERICAL SIMULATION

Consider a TGCS as follows [38]:

$$\begin{cases} \dot{x}_{1,k} = x_{2,k}, \\ \dot{x}_{2,k} = -\frac{R}{L}x_{2,k} - \frac{K_t K_e}{LJ}x_{1,k} + \frac{K_a K_t}{LJi}u_{q,k} \\ \qquad + \Delta f(\boldsymbol{x}_k, t), \end{cases} \tag{38}$$

where $R = 0.4\Omega$, $J = 5239\text{kg}\cdot\text{m}^2$, $i = 1039$, $L = 2.907 \times 10^{-3}$H, $K_t = 0.195N\cdot\text{m/A}$, $K_e = 0.197\ V/(\text{rad}\cdot s^{-1})$, $B = 1.43\times10^{-4}$ N$\cdot$m, $K_a = 2$, $\Delta f(\boldsymbol{x}_k, t) = 13.2 + 0.1\,x_{1,k} + 0.2\,x_{2,k} + 0.2\text{sign}(x_{2,k}) + 0.2\text{rand1}(k)\sin(0.5t)$, $T = 5$. The control objective is to make $\boldsymbol{x}_k$ accurately track its reference trajectory $\boldsymbol{x}_d = [0.5 + \sin(\frac{\pi}{2}t), \frac{\pi}{2}\cos(\frac{\pi}{2})]^T$ under the initial condition $\boldsymbol{x}_k(0) = [0.7 + 0.1\text{rand2}(k), 0.8 + 0.02\text{rand3}(k)]^T$. Here, rand1$(\cdot)$, rand2$(\cdot)$ and rand3$(\cdot)$ are random numbers between 0 and 1.

The adaptive ILC law (7) and adaptive learning laws (8)-(9) are adopted for this simulation with $T_1 = 0.6$, $T = 5$, $\alpha = 2$, $\varepsilon = 0.02$, $\gamma_1 = 10$, $\gamma_2 = 3$, $\gamma_3 = 0.03$, $\underline{\theta} = -30$, $\bar{\theta} = 30$, $\bar{\eta} = 10$. The number of RBF network neurons in (12) is chosen to be $m = 7$, with $\boldsymbol{c}_j$ evenly spaced on $[-3, 3] \times [-3, 3] \times [-3, 3] \times [-3, 3] \times [-3, 3] \times [-3, 3] \times [-3, 3]$ and the correspondent width $b_j = 4$ for $j = 1, 2, \cdots, 7$.

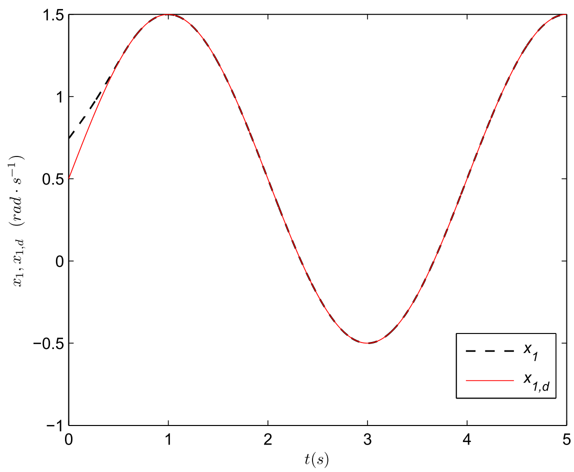


**FIGURE 3.** $\boldsymbol{x_1}$ **and its reference signal** $\boldsymbol{x_{1,d}}$.

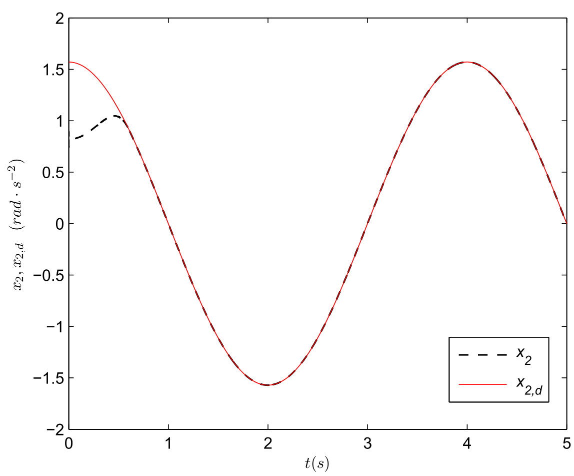


**FIGURE 4.** $\boldsymbol{x_2}$ **and its reference signal** $\boldsymbol{x_{2,d}}$.

After 50 iteration cycles, the simulation results are given in Figs. 3–10. Figs. 3-4 present the state profiles at the 50th iteration. The profiles of state tracking error and reference error trajectory are shown in Figs. 5-6, with the corresponding difference between state error and reference error trajectory being presented in Figs 7-8. From Figs 5-8, we can see $\boldsymbol{e}_k(t)$ can precisely track $\boldsymbol{e}_k^*(t)$ over $[0, T]$ as the iteration number increases. According to Figs. 3–6, we conclude that $\boldsymbol{x}_k(t)$ can precisely track $\boldsymbol{x}_d(t)$ over $[T_1, T]$ as the iteration number increases. The profile of control input at the 50th iteration is shown in Fig. 9. Fig. 10 gives the convergence history of $s_{z,k}$, where $J_k \triangleq \max_{t\in[0,T]} |s_{z,k}(t)|$.

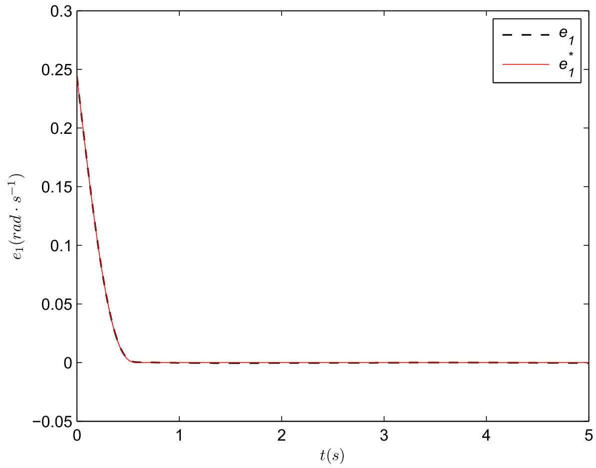


**FIGURE 5.** $\boldsymbol{e_1}$ **and** $\boldsymbol{e_1^*}$.

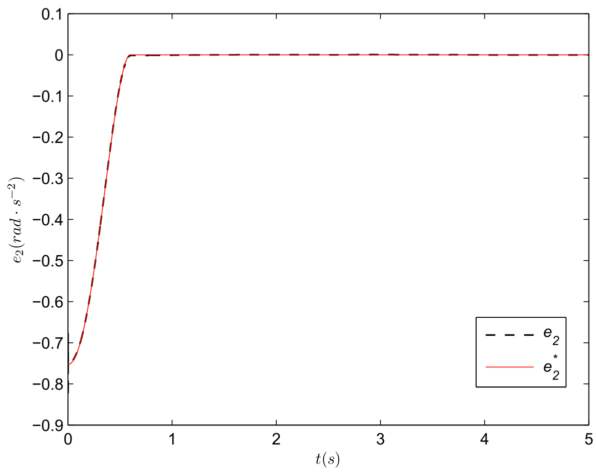


**FIGURE 6.** $\boldsymbol{e_2}$ **and** $\boldsymbol{e_2^*}$.

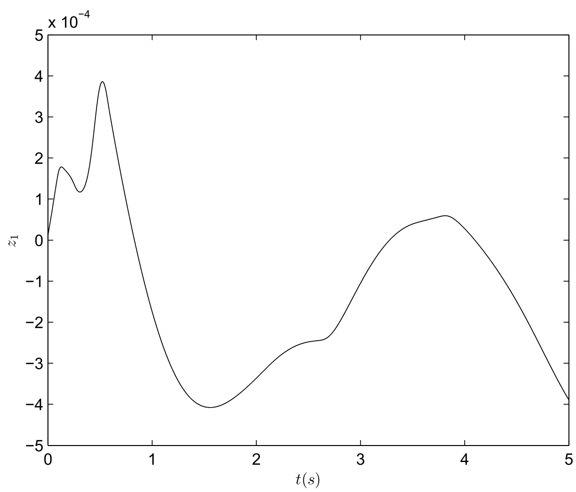


**FIGURE 7.** **The signal** $\boldsymbol{z_1}$.

For comparison, the robust adaptive ILC algorithm (39)-(41) proposed in [21] will be simulated for (38).

$$u_{q,k} = -\gamma_4 s_{\varpi k} - \boldsymbol{p}_k^T \boldsymbol{\varphi}_k - \boldsymbol{\vartheta}_k^T \boldsymbol{\psi}_k, \tag{39}$$

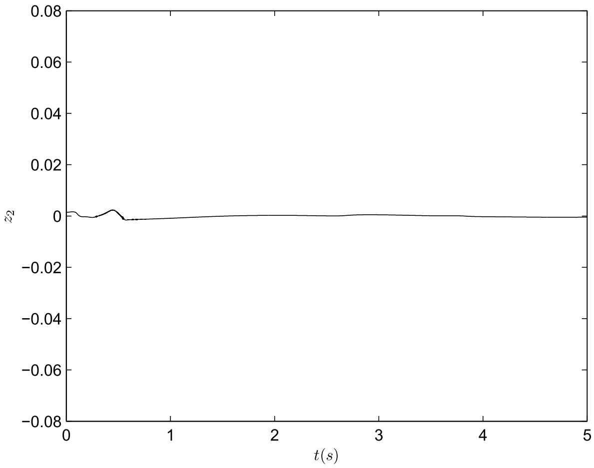


**FIGURE 8.** The signal $z_2$.

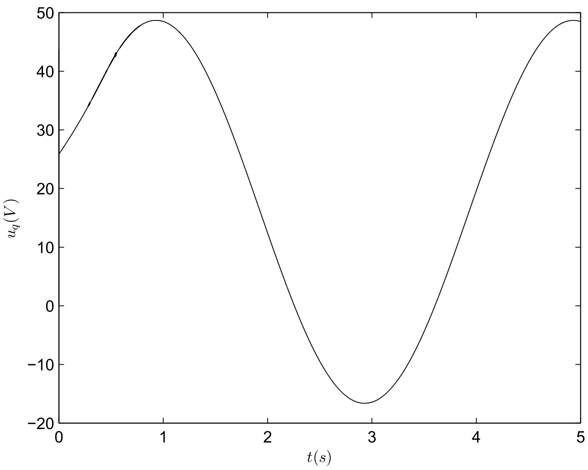


**FIGURE 9.** Control input.

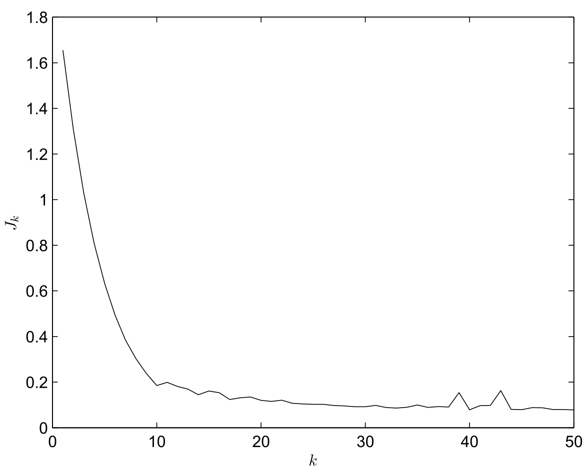


**FIGURE 10.** History of $s_{z,k}$ convergence.

$$\boldsymbol{p}_k = \mathrm{sat}_{\underline{p},\bar{p}}(\boldsymbol{p}_{k-1}) + \gamma_5 s_{\varpi k}\boldsymbol{\varphi}_k, \quad \boldsymbol{p}_{-1} = 0, \tag{40}$$

$$\boldsymbol{\vartheta}_k = \mathrm{sat}_{\underline{\vartheta},\bar{\vartheta}}(\boldsymbol{\vartheta}_{k-1}) + \gamma_6 s_{\varpi k}\boldsymbol{\psi}_k, \quad \boldsymbol{\vartheta}_{-1} = 0. \tag{41}$$

where, $s_k = \alpha e_{1,k} + e_{2,k}$, $s_{\varpi k} = s_k - \varpi\,\mathrm{sat}(\frac{s_k}{\varpi})$, $\boldsymbol{\varphi}_k \triangleq [ce_{2,k} - \ddot{x}_d, x_{2,k}, x_{1,k}, 1]^T$, $\boldsymbol{\psi}_k \triangleq [\|\boldsymbol{e}_k\|\mathrm{sat}_{-1,1}(\frac{s_k}{\varpi}),\ \mathrm{sat}_{-1,1}(\frac{s_k}{\varpi})]^T$, $\alpha = 2, \varpi = 0.02, \gamma_4 = 10, \gamma_5 = 3, \gamma_6 = 0.03, \underline{p} = -100, \bar{p} = 100, \underline{\vartheta} = -100, \bar{\vartheta} = -100$.

The intial states and other control parameters are the same as the ones in the previous simulation.

The maximum value of $|s_{\varpi,k}|$ at each cycle is illustrated in Fig. 11, where $J_{s,k} \triangleq \max_{t\in[0,T]} |s_{\varpi,k}(t)|$. From Fig. 11, we can see that $J_{s,k}$ does not decrease as the iteration number inreases. Comparing Fig. 10 with Fig. 11, we conclude that the control scheme (39)-(41) is not suitable for TGCSs with arbitrary initial states.

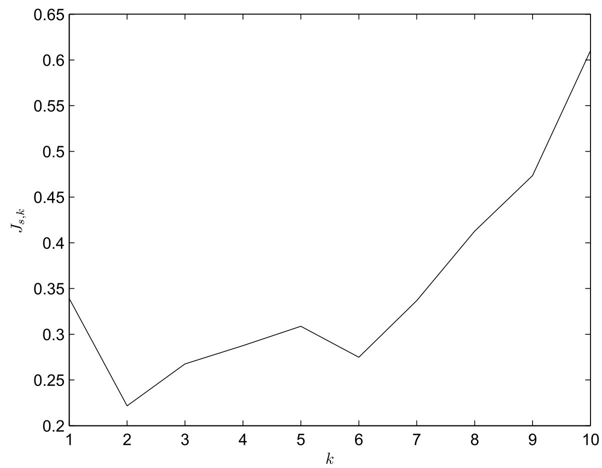


**FIGURE 11.** Maximum value of $|s_{\varpi,k}|$ at each cycle.

*Remark 3:* In fact, the above-mentioned robust adaptive ILC algorithm is suitable for TGCSs under alignment condition, i.e., while the reference trajectories of TGCSs are smoothly closed, $\boldsymbol{x}_{k+1}(0) = \boldsymbol{x}_k(T)$ may be used to solve the initial problem of ILC.

The above simulation results verify the effectiveness of the proposed neural network-based adaptive ILC scheme.

## VI. CONCLUSION

A neural network-based error-tracking ILC scheme has been proposed to solve the trajectory-tracking problem for TGCSs with arbitrary initial states. With the corresponding desired error trajectory being constructed, an error-tracking strategy is utilized to solve the initial problem of ILC. An adaptive iterative learning controller is designed by using Lyapunov approach, with adaptive learning RBF neural network used to approximate uncertainties. Simulation results have verified the effectiveness of the proposed neural network-based error-tracking ILC algorithm.

## REFERENCES

[1] S. Arimoto, S. Kawamura, and F. Miyazaki, "Bettering operation of robots by learning," *J. Robot. Syst.*, vol. 1, no. 2, pp. 123–140, 1984.

[2] M. French and E. Rogers, "Non-linear iterative learning by an adaptive Lyapunov technique," *Int. J. Control*, vol. 73, no. 10, pp. 840–850, Jan. 2000.

[3] J.-X. Xu and Y. Tan, "A composite energy function-based learning control approach for nonlinear systems with time-varying parametric uncertainties," *IEEE Trans. Autom. Control*, vol. 47, no. 11, pp. 1940–1945, Nov. 2002.

[4] C. Yin, J.-X. Xu, and Z. Hou, ''A high-order internal model based iterative learning control scheme for nonlinear systems with time-iteration-varying parameters,'' *IEEE Trans. Autom. Control*, vol. 55, no. 11, pp. 2665–2670, Nov. 2010.
[5] Y. Xudong, ''Nonlinear adaptive learning control with disturbance of unknown periods,'' *IEEE Trans. Autom. Control*, vol. 57, no. 5, pp. 1269–1273, May 2012.
[6] J.-X. Xu, X. Jin, and D. Huang, ''Composite energy function-based iterative learning control for systems with nonparametric uncertainties,'' *Int. J. Adapt. Control Signal Process.*, vol. 28, no. 1, pp. 1–13, Jan. 2014.
[7] Q. Yan and M. Sun, ''Suboptimal learning control for nonlinear systems with both parametric and nonparametric ncertainties,'' *Acta Automat. Sinica*, vol. 41, no. 9, pp. 1659–1668, 2015.
[8] H. Su, H. Zhang, X. Liang, and C. Liu, ''Decentralized event-triggered online adaptive control of unknown large-scale systems over wireless communication networks,'' *IEEE Trans. Neural Netw. Learn. Syst.*, early access, Jan. 13, 2020, doi: 10.1109/TNNLS.2019.2959005.
[9] H. Zhang, H. Su, K. Zhang, and Y. Luo, ''Event-triggered adaptive dynamic programming for non-zero-sum games of unknown nonlinear systems via generalized fuzzy hyperbolic models,'' *IEEE Trans. Fuzzy Syst.*, vol. 27, no. 11, pp. 2202–2214, Nov. 2019.
[10] H. Zhang, L. Cui, X. Zhang, and Y. Luo, ''Data-driven robust approximate optimal tracking control for unknown general nonlinear systems using adaptive dynamic programming method,'' *IEEE Trans. Neural Netw.*, vol. 22, no. 12, pp. 2226–2236, Dec. 2011.
[11] K. Zhang, H. Zhang, Y. Mu, and C. Liu, ''Decentralized tracking optimization control for partially unknown fuzzy interconnected systems via reinforcement learning method,'' *IEEE Trans. Fuzzy Syst.*, early access, Jan. 13, 2020, doi: 10.1109/TFUZZ.2020.2966418.
[12] K. Zhang, H.-G. Zhang, Y. Cai, and R. Su, ''Parallel optimal tracking control schemes for mode-dependent control of coupled Markov jump systems via integral RL method,'' *IEEE Trans. Autom. Sci. Eng.*, early access, Nov. 12, 2019, doi: 10.1109/TASE.2019.2948431.
[13] R. Dana and E. Kreindler, ''Variable structure control of a tank gun,'' in *Proc. 1st IEEE Conf. Control Appl.*, Sep. 1992, pp. 928–933.
[14] W. Grega, ''Time-optimal control of n-tank system,'' in *Proc. IEEE Int. Conf. Control Appl.*, Sep. 1998, pp. 522–526.
[15] S. Shao-Jian, C. Gang, L. Bi-Lian, and L. Xiao-Feng, ''Real-time optimal control for three-tank level system via improved ADDHP method,'' in *Proc. IEEE Int. Conf. Control Automat.*, Dec. 2009, pp. 564–568.
[16] T. Jin, H. S. Yan, and D. X. Li, ''PID control for tank firing in motion,'' *Ind. Control Comput.*, vol. 29, no. 7, pp. 18–19, 2016.
[17] N. Y. Li, K. C. Li, and Y. L. Liu, ''Investigation of direct adaptive controller for tank gun elevation control system,'' *J. Syst. Simul.*, vol. 23, no. 4, pp. 762–765, 2011.
[18] J. Cai, R. Yu, Q. Yan, C. Mei, B. Wang, and L. Shen, ''Event-triggered adaptive control for tank gun control systems,'' *IEEE Access*, vol. 7, pp. 17517–17523, 2019.
[19] L.-J. Shen and J. P. Cai, ''Adaptive robust control of gun control servo system of tank,'' *Math. Pract. Theory*, vol. 42, no. 7, pp. 170–175, 2012.
[20] Q. Yan, Y. Yu, Y. Ma, and J. Cai, ''Error-tracking iterative learning control for gun control servo system of tank,'' in *Proc. Int. Conf. Control, Automat. Inf. Sci. (ICCAIS)*, Hangzhou, China, Oct. 2018, pp. 361–366.
[21] G. Zhu, X. Wu, Q. Yan, and J. Cai, ''Robust learning control for tank gun control servo systems under alignment condition,'' *IEEE Access*, vol. 7, pp. 145524–145531, 2019.
[22] Y. Xia, L. Dai, M. Fu, C. Li, and C. Wang, ''Application of active disturbance rejection control in tank gun control system,'' *J. Franklin Inst.*, vol. 351, no. 4, pp. 2299–2314, Apr. 2014.
[23] J. H. Hu, Y. L. Hou, and Q. Gao, ''Sliding-mode control for tank gun controlling system based on disturbance observer,'' *Electron. Opt. Control*, vol. 25, no. 2, pp. 98–101, 2018.
[24] L. Feng, X. Ma, Z. Yan, and H. Li, ''Method of adaptive fuzzy sliding mode control of gun control system of tank,'' *Electr. Mach. Control*, vol. 11, no. 1, pp. 65–69, 2007.
[25] J. H. Hu, Y. L. Hou, and Q. Gao, ''Method of neural network adaptive sliding mode control of gun control system of tank,'' *Fire Control Command Control*, vol. 43, no. 6, pp. 118–121, 2018.
[26] J.-X. Xu and R. Yan, ''On initial conditions in iterative learning control,'' *IEEE Trans. Autom. Control*, vol. 50, no. 9, pp. 1349–1354, Sep. 2005.
[27] X. E. Ruan and J. Zhao, ''Pulse compensated iterative learning control to nonlinear systems with initial state uncertainty,'' *Control Theory Appl.*, vol. 29, no. 8, pp. 993–1000, 2012.
[28] Q. Z. Yan, M. X. Sun, and H. Li, ''Iterative learning control for nonlinear uncertain systems with arbitrary initial state,'' *Acta Automat. Sinica*, vol. 42, no. 4, pp. 545–555, 2016.
[29] C.-J. Chien, C.-T. Hsu, and C.-Y. Yao, ''Fuzzy system-based adaptive iterative learning control for nonlinear plants with initial state errors,'' *IEEE Trans. Fuzzy Syst.*, vol. 12, no. 5, pp. 724–732, Oct. 2004.
[30] L. Wu, Q. Yan, and J. Cai, ''Neural network-based adaptive learning control for robot manipulators with arbitrary initial errors,'' *IEEE Access*, vol. 7, pp. 180194–180204, 2019.
[31] M.-X. Sun and Q.-Z. Yan, ''Error tracking of iterative learning control systems,'' *Acta Automat. Sinica*, vol. 39, no. 3, pp. 251–262, Mar. 2014.
[32] Q. Yan and M. Sun, ''Error trajectory tracking by robust learning control for nonlinear systems,'' *Control Theory Appl.*, vol. 30, no. 1, pp. 23–30, Jan. 2013.
[33] Q. Z. Yan, M. X. Sun, and H. Li, ''Consensus-error-tracking learning control for nonparametric uncertain multi-agent systems,'' *Control Theory Appl.*, vol. 33, no. 6, pp. 793–799, 2016.
[34] X.-D. Li, M.-M. Lv, and J. K. L. Ho, ''Adaptive ILC algorithms of nonlinear continuous systems with non-parametric uncertainties for non-repetitive trajectory tracking,'' *Int. J. Syst. Sci.*, vol. 47, no. 10, pp. 2279–2289, Jul. 2016.
[35] Q. Z. Yan, M. X. Sun, and J. P. Cai, ''Filtering-error rectified iterative learning control for systems with input dead-zone,'' *Control Theory Appl.*, vol. 34, no. 1, pp. 77–84, 2017.
[36] Q. Z. Yan, M. X. Sun, and J. P. Cai, ''Reference-signal rectifying method of iterative learning Control,'' *Acta Automat. Sinica*, vol. 43, no. 8, pp. 1470–1477, 2017.
[37] W. E. Dixon, E. Zergeroglu, D. M. Dawson, and B. T. Costic, ''Repetitive learning control: A Lyapunov-based approach,'' *IEEE Trans. Syst., Man, Cybern. B. Cybern.*, vol. 32, no. 4, pp. 538–545, Aug. 2002.
[38] C. C. Sun, C. Jie, and L. Dou, ''Variable structure control for sliding mode of tank stabilizator based on optimization,'' *Acta Armamentaria*, vol. 22, no. 1, pp. 15–18, 2001.

**QIYAO YANG** received the B.S. degree in automation and the M.S. degree in control theory and control engineering from Hangzhou Dianzi University, Hangzhou, China, in 2002 and 2005, respectively, where he is currently pursuing the Ph.D. degree in control science and engineering with the School of Automation. Since 2005, he has been working as a Lecturer with the School of Electrical Engineering, Zhejiang University of Water Resources and Electric Power, Hangzhou. His current research interests include iterative learning control and artificial intelligence. He is a member of the Chinese Association of Automation.

**QIUZHEN YAN** received the M.S. degree in computer science and the Ph.D. degree in control science and engineering from the Zhejiang University of Technology, Hangzhou, China, in 2005 and 2015, respectively. Since 2005, he has been with the College of Information Engineering, Zhejiang University of Water Resources and Electric Power, where he is currently a Lecturer. His current research interests are mainly in iterative learning control and repetitive control. He is a Senior Member of the Chinese Association of Automation.

**JIANPING CAI** was born in 1975. He received the Ph.D. degree from Zhejiang University, in 2014. He is currently an Associate Professor with the Zhejiang University of Water Resources and Electric Power. His main research interests include nonlinear systems and adaptive control.

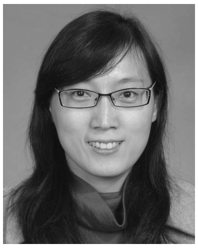

**JINGHUA TIAN** received the B.S. degree in computer science and technology from the Huazhong University of Science and Technology, in 2002, and the M.S. degree in communication and information system from the Zhejiang University of Technology. In 2004, she came to Zhejiang University of Water Resources and Electric Power. She held an Assistant position with the Information Engineering and Art Design Department, Hangzhou. Since 2004, she has been working as a Lecturer with the Zhejiang University of Water Resources and Electric Power. Her current research interests include automatic control, industrial automation, computer networking technology, and communication technology.

**XIAOHUI GUAN** received the master's degree in computer science from Zhejiang University, Hangzhou, China, in 2005. She is currently an Associate Professor with the College of Information Engineering, Zhejiang University of Water Resources and Electric Power. Her current research interests are in machine learning and adaptive control.